Cerebral Cortex May 2010;20:1195–1207
doi:10.1093/cercor/bhp180
Advance Access publication August 26, 2009

Representation of Neck Velocity and Neck–Vestibular Interactions in Pursuit Neurons in the Simian Frontal Eye Fields

Kikuro Fukushima[1], Teppei Akao[1], Hiroshi Saito[1,2], Sergei A. Kurkin[1], Junko Fukushima[2] and Barry W. Peterson[3]

[1]Department of Physiology, [2]Department of Health Sciences, Hokkaido University School of Medicine, Sapporo 060-8638, Japan and [3]Northwestern University Medical School, Chicago, IL 60611, USA

The smooth pursuit system must interact with the vestibular system to maintain the accuracy of eye movements in space (i.e., gaze-movement) during head movement. Normally, the head moves on the stationary trunk. Vestibular signals cannot distinguish whether the head or whole body is moving. Neck proprioceptive inputs provide information about head movements relative to the trunk. Previous studies have shown that the majority of pursuit neurons in the frontal eye fields (FEF) carry visual information about target velocity, vestibular information about whole-body movements, and signal eye- or gaze-velocity. However, it is unknown whether FEF neurons carry neck proprioceptive signals. By passive trunk-on-head rotation, we tested neck inputs to FEF pursuit neurons in 2 monkeys. The majority of FEF pursuit neurons tested that had horizontal preferred directions (87%) responded to horizontal trunk-on-head rotation. The modulation consisted predominantly of velocity components. Discharge modulation during pursuit and trunk-on-head rotation added linearly. During passive head-on-trunk rotation, modulation to vestibular and neck inputs also added linearly in most neurons, although in half of gaze-velocity neurons neck responses were strongly influenced by the context of neck rotation. Our results suggest that neck inputs could contribute to representing eye- and gaze-velocity FEF signals in trunk coordinates.

Keywords: coordinate frame, frontal eye fields, monkey, neck proprioception, smooth pursuit, vestibular system

Introduction

To obtain accurate visual information about slowly moving objects, smooth pursuit eye movements are essential and are made in response to visual information about the velocity of slip of the object's image on the retina. During movement of the whole body, the smooth pursuit system must interact with the vestibular system to maintain the target image on the fovea for accurate pursuit eye movements in space (i.e., gaze movement). Neural signals representing image motion on the retina, the velocity of head rotation, and pursuit eye velocity are used to compute an estimate of target velocity in space which is eventually converted into gaze-velocity (see Leigh and Zee 2006 for a review). In daily life, the head usually moves on the stationary trunk. The vestibular system cannot distinguish whether the head is moving by itself or if the whole body is moving. This distinction must depend on neck proprioceptive afferents that provide information about head movements relative to the trunk (e.g., Mergner et al. 1992). Moreover, in situations where subjects make an aiming movement toward a target that moves with their body, pursuit eye movements must be coordinated with hand and/or arm movements for accurate motor performance (Maioli et al. 2007). Such coordination would require representation of pursuit command signals with respect to the trunk. For this, neck proprioceptive information would also be needed.

The caudal part of the frontal eye fields (FEF) in the fundus of the arcuate sulcus has been known to contain neurons that discharge in relation to ocular smooth pursuit in head-fixed monkeys (pursuit neurons), and these neurons are thought to generate a pursuit command (MacAvoy et al. 1991; Gottlieb et al. 1993, 1994; Tanaka and Fukushima 1998; Akao et al. 2005; Kurkin et al. 2009). The majority of FEF pursuit neurons carry not only visual information about the velocity of target motion, but also vestibular information about the direction of whole-body rotation and translation, and signal eye- or gaze-velocity (Fukushima et al. 2000; Fukushima, Yamanobe, Shinme, Fukushima, 2002; Akao et al. 2007, 2009; Fukushima, Kasahara, Akao, Kurkin, et al., 2009). However, it is unknown whether FEF pursuit neurons carry neck proprioceptive signals and if so, how neck proprioceptive responses interact with smooth pursuit and vestibular responses. These are the questions we address in the present study.

By applying passive rotation of the trunk under the stationary head while monkeys fixated a stationary spot in space to minimize contribution of gaze movement–related discharge, we have now shown that the great majority of FEF pursuit neurons do indeed signal neck velocity. Neck velocity responses and pursuit responses added linearly. During passive head-on-trunk rotation, discharge modulation to vestibular and neck inputs also added linearly in most neurons, although in a group of FEF pursuit neurons neck responses were strongly influenced by the context in which neck rotation occurred. Some of the results were presented in preliminary form (Fukushima et al. 2007; Fukushima, Kasahara, Akao, Saito, et al., 2009).

Materials and Methods

Two monkeys (Sh, Si, *Macaca fuscata*, 3.5 and 4.5 kg) were used. All procedures were performed in strict compliance with the guidelines for the Care and Use of Animals of National Institutes of Health. Specific protocols were approved by the Animal Care and Use Committee of Hokkaido University School of Medicine. Methods for animal preparation, training, recording, and data analysis were basically similar to those in previous studies (Fukushima et al. 2000; Akao et al. 2005; Kasahara et al. 2006; Fukushima, Kasahara, Akao, Kurkin, et al., 2009), except for trunk rotation, and are summarized here briefly. Each monkey was sedated with ketamine hydrochloride (5 mg/kg, i.m.), and then anesthetized with pentobarbital sodium (25 mg/kg, i.p.). Under aseptic conditions, head holders were installed to restrain the head firmly in the primate chair in the stereotaxic plane. Vertical and horizontal components of eye movements were recorded by the scleral search coil method (Fuchs and Robinson 1966). The monkeys were

© 2009 The Authors
This is an Open Access article distributed under the terms of the Creative Commons Attribution Non-Commercial License (http://creativecommons.org/licenses/by-nc/2.5/uk/) which permits unrestricted non-commercial use, distribution, and reproduction in any medium, provided the original work is properly cited.

rewarded with apple juice for tracking or fixating a target spot. A recording chamber was installed over a craniotomy aiming at Ant. 23 and Lat. 15 stereotaxic coordinates to enable single neuron recording in the left periarcuate sulcus region as described previously (e.g., MacAvoy et al. 1991; Tanaka and Fukushima 1998; Fukushima et al. 2000; Fukushima, Yamanobe, Shinme, Fukushima 2002; Akao et al. 2007, 2009).

Recording Procedures

Extracellular recordings were made in the left periarcuate sulcus region to locate neurons related to pursuit of a moving target spot as reported previously (MacAvoy et al. 1991; Gottlieb et al. 1993, 1994; Tanaka and Fukushima 1998; Fukushima et al. 2000; Fukushima, Yamanobe, Shinme, Fukushima, 2002; Fukushima, Yamanobe, Shinme, Fukushima, Kurkin, et al. 2002; Akao et al. 2005; Fukushima, Kasahara, Akao, Kurkin, et al., 2009). Once an isolated neuron responding during pursuit was encountered, smooth pursuit responses were tested in 4 planes (vertical, horizontal and 2 oblique planes at 45° angles) to determine the preferred direction. Figure 1*A–E* schematically summarizes the stimulus conditions. Once single neurons responding to horizontal smooth pursuit were isolated (Fig. 1*A*), the monkeys were tested under 4 additional task conditions (Fig. 1*B–E*); passive trunk rotation while the head was held stationary in space facing a computer screen straight ahead of the monkeys' eyes (Fig. 1*B*, trunk-on-head rotation), passive whole-body rotation (Fig. 1*C,D*), and passive rotation of the head while the trunk was held stationary in space (Fig. 1*E*, head-on-trunk rotation).

The animal's trunk was restrained by polystyrene foam in the primate chair so that chair rotation securely rotated the trunk (Kasahara et al. 2006). A single horizontal motor was used to apply passive trunk-on-head rotation, passive whole-body rotation, and passive head-on-trunk rotation so that the same horizontal rotation was applied along the identical vertical axis in the 3 task conditions. A position signal of horizontal rotation was obtained from a potentiometer attached to the common motor. During passive head-on-trunk rotation, horizontal head movement was also recorded by another potentiometer attached to the shaft of the vertical axis to confirm that head movement was identical to the potentiometer output of the common motor. During passive trunk-on-head rotation, a mechanical lock was attached to the shaft so that the head could be stabilized in space and only the trunk was rotated. Similarly, during passive head-on-trunk rotation, the chair was stabilized in space by another mechanical lock, thus allowing only the head to be rotated.

During trunk-on-head rotation (Fig. 1*B*) and head-on-trunk rotation (Fig. 1*E*), the target stayed stationary in space straight ahead of the monkeys' eyes to minimize the contribution of gaze movement–related discharge modulation. During passive trunk-on-head rotation (Fig. 1*B*), the direction of head rotation relative to the trunk (i.e., neck movement) is opposite to the direction of trunk rotation in space as indicated (head-retrunk, Fig. 1*B*). During passive whole-body rotation and passive head-on-trunk rotation (Fig. 1*C–E*), the juice feeder was moved together with the head.

Passive rotation was applied sinusoidally at 0.3 Hz (±10°, peak velocity 18.8°/s, Fig. 1*B–E*). We also applied trunk-on-head rotation at different frequencies with constant amplitude (0.2–1.0 Hz, ±10°, peak trunk velocity 12.5–62.8 °/s). In addition, we applied trunk-on-head rotation in a ramp trajectory (at 20°/s, ±10°) with random intertrial intervals (1–3 s) to examine velocity and/or position-related response and latency of discharge modulation. In these conditions, the signal from the potentiometer attached to the shaft of the vertical axis continuously monitored head rotation and we confirmed that the head did not move in space during trunk-on-head rotation.

To examine the interaction of smooth pursuit and trunk-on-head rotation responses, we tested discharge modulation when the target moved together with the trunk with the same direction and amplitudes (e.g., Fig. 6*B*). The number of neurons tested varied between task conditions due to the occasional degradation or loss of neural recordings. For some neurons with vertical or oblique pursuit preferred directions, trunk-on-head rotation was also tested for comparison (Results not shown).

During passive whole-body rotation we further tested 2 conditions to classify pursuit neurons either as gaze-velocity or as eye/head-velocity neurons as described previously (Fukushima et al. 2000; Akao et al. 2007). This was to examine a possible difference in neck proprioceptive responses and their interaction with vestibular responses. In one, the monkeys were required to fixate a stationary spot in space during whole-body rotation by a perfect vestibulo-ocular reflex (VOR) so that gaze remained stationary in space (VOR ×1, Fig. 1*C*). In the other, the monkeys were required to track a target that moved in space with the whole-body rotation (Fig. 1*D*). This condition required the monkeys to cancel the VOR so that the eyes remained relatively motionless in the orbit and gaze moved together with the whole body. Based on the previous criteria (Fukushima et al. 2000; Akao et al. 2007), we classified pursuit neurons as gaze-velocity, if 1) their peak modulation occurred for eye (pursuit) and head (VOR cancellation) movements in the same direction; and 2) modulation was lower during VOR ×1 than during VOR cancellation. The pursuit neurons that responded to whole-body rotation but that did not meet the above criteria were classified as eye/head-velocity neurons, because such neurons basically coded eye velocity during VOR ×1 in previous studies (e.g., Lisberger and Fuchs 1978).

Data Analysis

Eye, target, and chair position signals and their derivatives were low-pass filtered (250 Hz) and digitized at 500 Hz. Neuronal discharge was discriminated, detected at 100 kHz, and stored in temporal register with analog signals. Saccades were marked with a cursor on eye velocity traces and removed using the interactive computer program as described previously (Singh et al. 1981; Fukushima et al. 2000). Cycle histograms were constructed by averaging discharge of each neuron

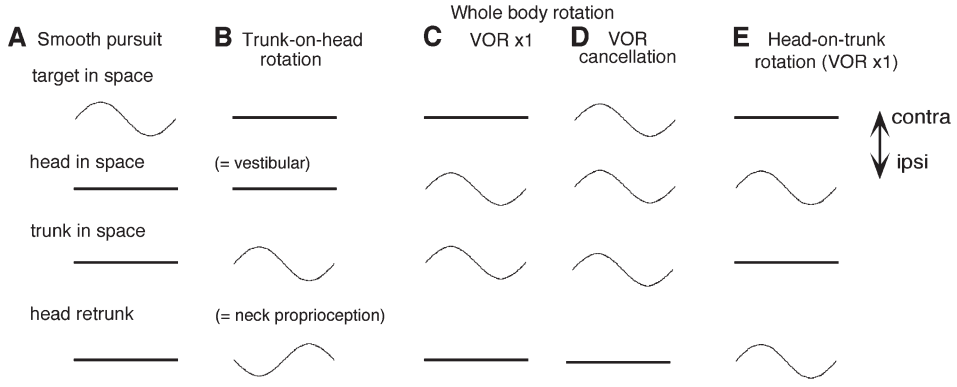

Figure 1. Task conditions during different types of stimulation. Task conditions are schematically shown for smooth pursuit (*A*), passive trunk-on-head rotation (*B*), passive whole-body rotation while the target was stationary in space (VOR ×1, *C*), passive whole-body rotation while the target moved together with the whole body (VOR cancellation, *D*), and passive head-on-trunk rotation (VOR ×1, *E*). See text for further explanation.

over 10–30 cycles. To quantify neuronal responses, each cycle was divided into 128 equal bins (e.g., Wilson et al. 1984). A sine function was fit to averaged velocities and cycle histograms of discharge of individual neurons, excluding the bins with zero spikes, by means of a least squared error algorithm. Signal-to-noise (S/N) ratio of the response was defined as the ratio of amplitude of the fit fundamental frequency component to the root mean square amplitude of the third through eighth harmonics. Harmonic distortion (HD) was defined as the ratio of the amplitude of the second harmonic to that of the fundamental according to Wilson et al. (1984). Responses with HD $\leq$ 50% or S/N $\geq$ 1.0 were accepted for further analysis. Sensitivity (restimulus velocity) was calculated as the peak amplitude of the fundamental component fitted to the cycle histogram divided by the peak amplitude of the fitted stimulus velocity. For those neurons that satisfied HD and S/N criteria, sensitivity (restimulus velocity) $\geq$ 0.10 sp/s/°/s was taken as significant modulation (e.g., Fukushima et al. 2000).

Amplitude of discharge modulation was calculated as the peak amplitude of the fundamental component fit to the cycle histograms. Phase shifts were measured between the peak of the fundamental component of the response and the peak contralateral (i.e., rightward) stimulus velocity. As the stimulus velocity, trunk velocity was used for trunk-on-head rotation (Fig. 1*B*), and head-velocity in space was used for whole-body rotation and head-on-trunk rotation (Fig. 1*C*–*E*).

To examine the latency of neuronal discharge in response to ramp trunk-on-head rotation, we first aligned 20–40 trials on the stimulus onset. Because discharge may have been affected by saccades, we then omitted all traces in which saccades appeared within ~100 ms of the stimulus onset (e.g., Fig. 17A2, C2 of Fukushima et al. 2000). The control values (mean and standard deviations, SD) before the onset of stimulus were calculated from the 200-ms interval immediately before the stimulus onset. Onset of the neuronal response to the onset of stimulus velocity was determined as the time at which the mean discharge rate in the histogram exceeded 2SD of the control value (e.g., Akao et al. 2005).

Histological Procedures

Near the conclusion of recordings in one monkey (Si), the sites of pursuit neuron recordings were marked by electrolytic lesions by passing current through the microelectrode. The monkey was deeply anesthetized with sodium pentobarbital (50 mg/kg, i.p.) and perfused with physiological saline followed by 3.5% formalin. After histological fixation, coronal sections were cut at 100-μm thickness on a freezing microtome. The sections were stained for cell bodies and fibers, and the locations of recording sites were verified as described previously (e.g., Tanaka and Fukushima 1998; Fukushima et al. 2000; Fukushima, Yamanobe, Shinme, Fukushima, 2002; Fukushima, Kasahara, Akao, Kurkin, et al., 2009; Akao et al. 2009).

Results

Discharge of FEF Pursuit Neurons during Passive Trunk Rotation under the Stationary Head

To examine whether FEF pursuit neurons receive neck proprioceptive inputs, we tested effects of sinusoidal horizontal trunk rotation (i.e., trunk-on-head rotation, Fig. 1*B*) on a total of 115 pursuit neurons that were recorded in the caudal FEF in 2 monkeys. Of the 115, 46 neurons were recorded in monkey Sh and 69 neurons were recorded in monkey Si. Seventy-nine of the 115 neurons had horizontal preferred directions during smooth pursuit (Fig. 1*A*), and the majority of these (69/79 = 87%) responded to horizontal trunk-on-head rotation. Thirty-six pursuit neurons had vertical or oblique preferred directions and only a minority of them (6/36 = 17%) were activated by horizontal trunk-on-head rotation. These results suggest that FEF pursuit neurons receive direction-specific inputs during trunk-on-head rotation. Discharge characteristics of pursuit neurons to trunk-on-head rotation in 2 monkeys were similar.

Among the horizontal pursuit neurons that responded to horizontal trunk-on-head rotation, the great majority (59/69 = 86%) exhibited a directional response (i.e., they were activated either during trunk-on-head rotation towards or away from the recording side). Only 14% (10 neurons) exhibited bidirectional modulation during trunk-on-head rotation. The 2 columns in Figure 2 illustrate discharge of 2 representative FEF pursuit neurons to the 5 stimulus conditions illustrated in Figure 1*A*–*E*. Neurons were selected because they responded during smooth pursuit (Fig. 2*A*). Figure 2*B* shows responses to the trunk-on-head rotation paradigm (Fig. 1*B*) during which the head remained fixed in space and the monkeys fixated a stationary spot straight in front of the fixed head to minimize contribution of smooth pursuit-related modulation. Even without the presence of a target, discharge modulation comparable to that during fixation of the stationary spot was clearly seen during trunk-on-head rotation (Fig. 3*A*). In both conditions, eye velocity responses (i.e., cervico-ocular reflex, Leigh and Zee 2006) were minimal (gain = eye velocity/trunk-on-head rotation velocity < 0.1, Fig. 2*B*), indicating that the modulation was not due to eye movement responses but was induced most probably by neck proprioceptive afferents (see Discussion).

To rule out the possibility that the modulation of these neurons during trunk-on-head rotation was induced by tactile afferents of the neck skin, we applied tactile stimulation to the skin by our hands and a small brush during recording of responsive neurons when the monkeys fixated a stationary spot. None of the tested neurons (n = 10) exhibited a clear response.

Neck Velocity Responses of FEF Pursuit Neurons

To examine whether responses to trunk-on-head rotation reflected primarily velocity- or position components of head movements relative to the trunk, trunk-on-head rotation was applied at different frequencies (0.2–1.0 Hz) with constant amplitude (±10°, peak trunk-on-head velocity 12.5–62.8 °/s). Figure 3*A* illustrates discharge of a representative pursuit neuron at different frequencies of trunk-on-head rotation. The response magnitudes clearly increased as peak trunk-on-head velocity increased from 0.3 to 1.0 Hz. Amplitude of discharge modulation of 22 FEF pursuit neurons tested is plotted against frequency of trunk-on-head rotation and peak trunk-on-head velocity in Figure 3*B*. There was a significant positive correlation between amplitude of discharge modulation and peak trunk-on-head velocity. The mean slope for the linear regression was 0.16 sp/s/°/s (n = 22).

Ten of the 22 neurons were tested without a target in complete darkness (e.g., Fig. 3*A*, no target). Figure 3*C* plots amplitude of discharge modulation of the 10 neurons against peak trunk-on-head velocity. A significant positive correlation was observed between the 2 without a visual target, similar to that with a stationary target (Fig. 3*C* vs. *B*).

The averaged discharge of a population of 32 pursuit neurons taken from the group of 59 neurons that exhibited directional response during 0.3-Hz trunk-on-head rotation with a stationary target is illustrated in Figure 3*D*. These neurons increased discharge modulation during trunk-on-head rotation towards the recording side. The peak discharge modulation was observed between peak trunk-on-head velocity and position, suggesting that the modulation contained both velocity and position components.

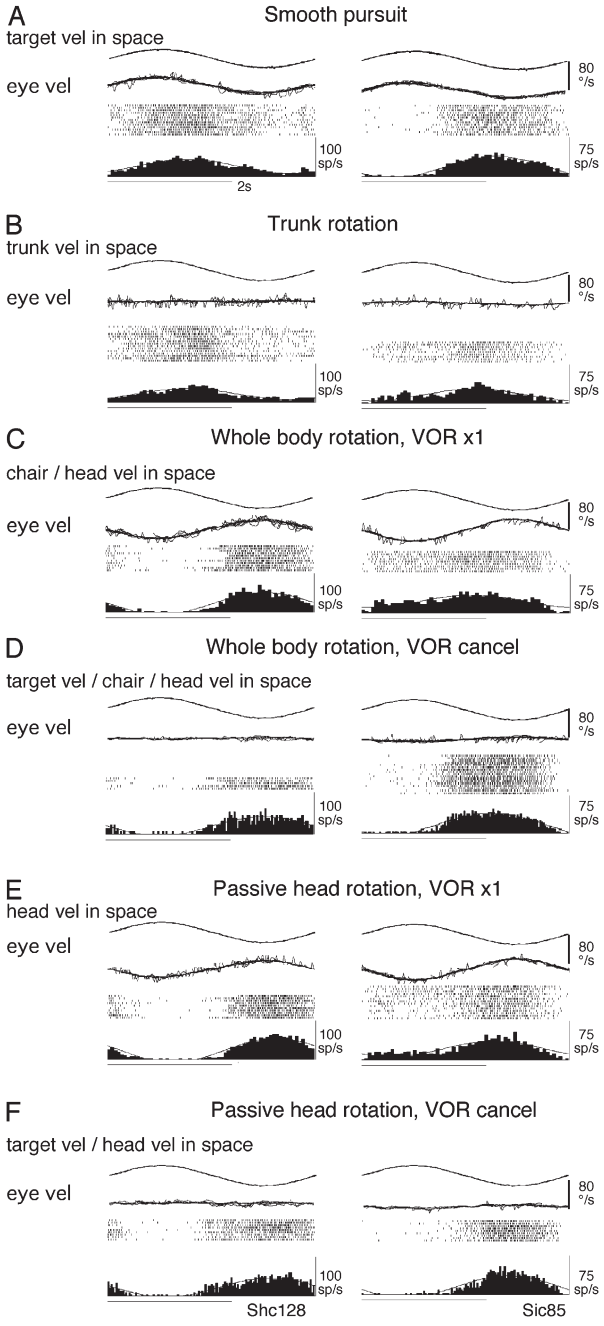

Figure 2. Discharge modulation of 2 representative FEF pursuit neurons during different task conditions. In *A–F*, discharge of gaze-velocity neuron (right column) and eye/head-velocity neuron (left column) is shown. These neurons were recorded in different monkeys. In each, the bottom 3 traces are de-saccaded eye velocity, spike rasters, and averaged histograms of neuronal discharge with superimposed fit sine waves. (*A*) Smooth pursuit. (*B*) Passive trunk-on-head rotation. (*C*) Passive whole-body rotation with an earth-stationary target (VOR ×1). (*D*) Passive whole-body rotation while the target moved together with the whole-body (VOR cancellation). (*E*) Passive head-on-trunk rotation with an earth-stationary target (VOR ×1). (*F*) Passive head-on-trunk rotation while the target moved together with the head (VOR cancellation). Vel and pos are velocity and position, respectively.

To examine this possibility further, a total of 53 neurons were also observed during velocity step trunk-on-head rotation at 20 °/s during fixation of a stationary spot (Fig. 4*A*). The majority of tested neurons (45/53 = 85%) exhibited velocity-related discharge modulation. Responses of 2 representative neurons are shown Figure 4*B*. The neuron illustrated in Figure 4*B* (top) exhibited discharge modulation only during velocity step trunk-on-head rotation; it showed initial burst discharge followed by steady discharge, whereas the neuron shown in Figure 4*B* (bottom) exhibited a steady velocity response followed by a position response during maintenance of a different trunk position relative to the stationary head (Fig. 4*A*). Three neurons (3/53 = 6%) responded only during maintenance of trunk-on-head position (not shown). The responses of the remaining 5 neurons varied: biphasic modulation (n = 3), pause during acceleration phase (n = 1), and burst only during acceleration phase (n = 1). Figure 4C illustrates mean (±SE) discharge of the population of 53 neurons showing a predominant velocity response. These results indicate that the discharge modulation during trunk-on-head rotation was predominantly a neck velocity response, while in addition, a minority of neurons exhibited modulation during acceleration and position phases as well (see Discussion).

Figure 4*D* summarizes latency distribution of the 45 responsive neurons. The modal latency was 35 ms with the median at 61 ms. These latencies are longer than vestibular responses induced by passive whole-body step rotation (=20 ms, Akao et al. 2007) but shorter than the typical visual responses of FEF pursuit neurons induced by target motion (~70–80 ms, see Leigh and Zee 2006 for a review).

Comparison of Discharge Modulation during Smooth Pursuit and Trunk-on-Head Rotation

By testing how vestibular responses interact with discharge modulation during smooth pursuit, previous studies have classified FEF pursuit neurons as either gaze-velocity neurons or eye/head-velocity neurons (Fukushima et al. 2000; Akao et al. 2007). To examine a possible difference in neck velocity responses and in their interaction with vestibular responses, in this study we classified a total of 66 FEF pursuit neurons as 1 of the 2 groups (Fig. 1*C,D*, see Recording procedures). Briefly, gaze-velocity neurons exhibited similar discharge modulation during smooth pursuit and VOR cancellation (*Fig. 1A,D*).

Of the 66 FEF pursuit neurons, 33 were classified as gaze-velocity neurons and the remaining 33 were classified as eye/head-velocity neurons (see Recording procedures, also Fukushima et al. 2000; Akao et al. 2007). Neck velocity responses were observed in both groups of neurons with similar percentage (31/33 of gaze-velocity neurons and 30/33 of eye/head-velocity neurons) and with similar amplitudes (mean ± SD, 9.3 ± 5.8 and 9.6 ± 6.7 sp/s, respectively). In Figure 2*A–E*, the neuron shown on the right was classified as a gaze-velocity neuron, and the neuron shown on the left was classified as an eye/head-velocity neuron. The neuron shown on the right exhibited similar discharge modulation during smooth pursuit (Fig. 2*A*) and VOR cancellation (Fig. 2*D*), and those response magnitudes were larger than that during VOR ×1 (Fig. 2*C*). In contrast, the neuron shown on the left reversed response phase during smooth pursuit (Fig. 2*A*) and VOR cancellation (Fig. 2*D*). In addition, the response magnitude during VOR ×1 (Fig. 2*C*) was slightly larger than that during VOR cancellation (Fig. 2*D*).

Linear Addition of Discharge Modulation during Smooth Pursuit and Trunk-on-Head Rotation

To examine how discharge modulation during smooth pursuit is affected by passive trunk-on-head rotation, we first tested whether there was any correlation in discharge modulation of

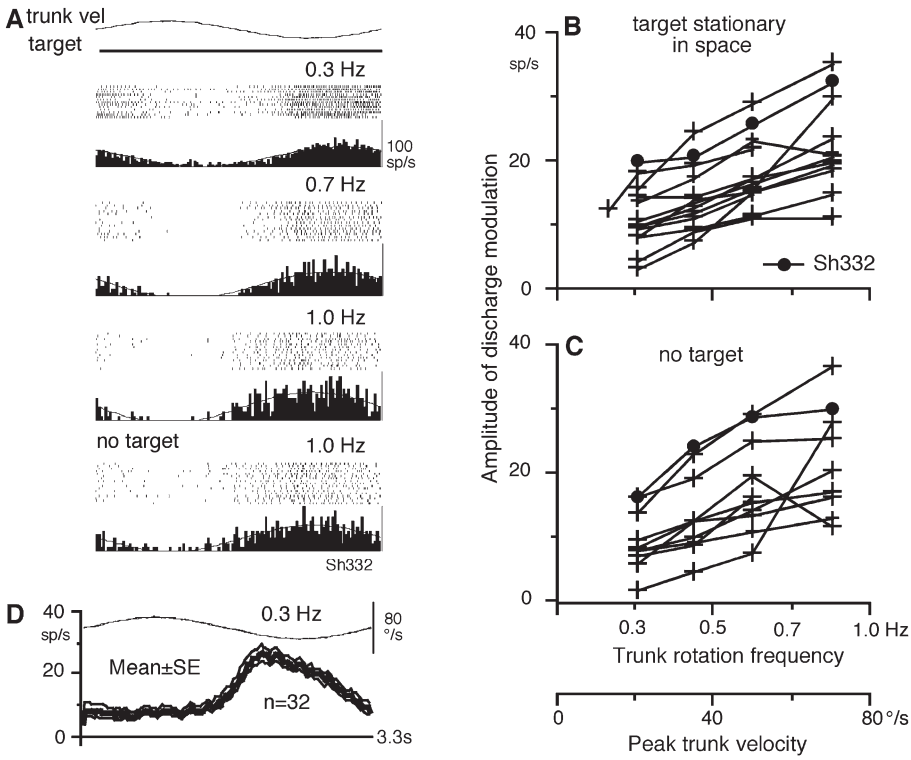

Figure 3. Responses of FEF pursuit neurons to passive trunk-on-head rotation. (*A*) Discharge of a single neuron during trunk-on-head rotation at increasing stimulus frequencies with constant amplitude (±10°). No target indicates that trunk-on-head rotation was applied in complete darkness without a target. (*B* and *C*) Amplitude of discharge modulation plotted against peak trunk-on-head velocity. In (*B*), the monkeys fixated a stationary spot in space; in (*C*), trunk-on-head rotation was applied in complete darkness without a target. Responses of each neuron are connected by lines. (*D*) Mean ± SE discharge of population of 32 pursuit neurons during passive trunk-on-head rotation at 0.3 Hz while the monkeys fixated a stationary spot in space.

individual horizontal pursuit neurons during smooth pursuit and trunk-on-head rotation (Fig. 1*A*,*B*). Figure 5*A*,*B* plot phase (relative to head–retrunk velocity, see Fig. 1*B*) and amplitude of modulation of the 66 neurons during trunk-on-head rotation against phase (retarget velocity) and amplitude of modulation during smooth pursuit. Their responses were distributed widely, and there was no correlation between the responses during the 2 task conditions in either group of neurons, suggesting independence of discharge modulation during the 2 task conditions (Fig. 5*A*,*B*).

In 36 FEF pursuit neurons we applied passive trunk-on-head rotation during smooth pursuit. These 2 responses added linearly. Figure 6*A*–*D* illustrates responses of a representative neuron. Discharge modulation when target motion and trunk rotation were applied separately (Fig. 6*A*) is shown in Figure 6*C* (black and blue, respectively), whereas Figure 6*D* (green) shows modulation when the 2 were applied together (Fig. 6*B*). Resting discharge rate was subtracted from the predicted discharge. The actual modulation during the latter condition (Fig. 6*D*, green) was clearly larger than each modulation (Fig. 6*C*), and was similar to the predicted modulation that was calculated by simply adding each modulation (Fig. 6*D*, red).

Figure 6*E* and *F* illustrates mean (±SE) discharge of 10 neurons that exhibited peak discharge near contralateral target velocity during pursuit and that also increased discharge during contralateral trunk rotation (Fig. 6*E*, black and blue, respectively). The actual modulation when target motion and trunk-on-head rotation were applied together (Fig. 6*F*, green) was similar to the modulation (Fig. 6*F*, red) predicted by summing the 2 responses (Fig. 6*E*). For the entire 36 neurons, we compared response phase (restimulus velocity) and amplitude of modulation of actual and predicted responses and plotted the results in Figure 6*G*, *H*. For all neurons, whether they were gaze-velocity or eye/head-velocity neurons (Fig. 6*G*,*H*), actual modulation was well predicted by linear addition of each modulation. The correlation coefficients were high (r = 0.87–0.99) with regression slopes close to one (0.96–1.03).

Linear addition of discharge modulation during smooth pursuit and trunk-on-head rotation was also shown by testing discharge modulation during pursuit and trunk-on-head rotation at different frequencies. Discharge of a representative neuron is shown in Figure 7*A*–*D*. Smooth pursuit was tested at 0.7 Hz and trunk-on-head rotation was tested at 0.3 Hz (Fig. 7*A*,*B*). Modulation during combined stimulation (Fig. 7*C*) was predicted by the simple linear addition of each modulation (Fig. 7*D*, actual versus predicted (a + b)).

To evaluate how well the sum of individual modulation predicted the combined modulation for each neuron, we approximated actual modulation $R(t)$ by the predicted modulation $S(t)$ using the equation: $R(t) = G \times S(t - \tau) + B$, where $R(t)$ is discharge rate at time t during combined stimulation; $S(t)$ is sum of discharge during smooth pursuit alone $E(t)$ and trunk rotation alone $T(t)$; τ is a time shift between predicted and actual responses; G is a gain factor; and B is a bias term for the difference in DC rate between predicted and actual responses. Figure 7*D* shows the least squares fit result for the example neuron (Fig. 7*A*-C). The best fit was achieved at gain G = 0.70

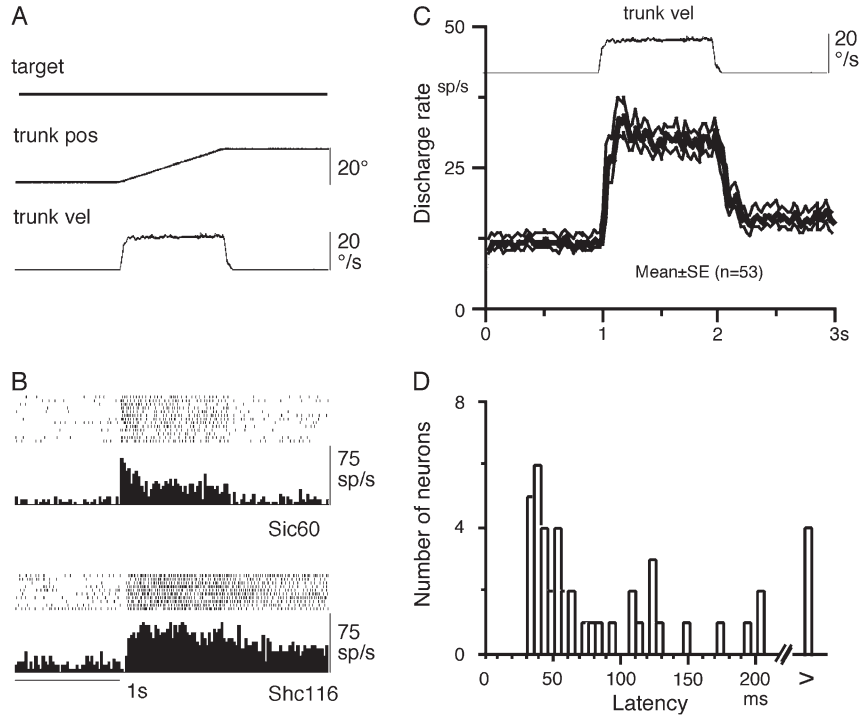

Figure 4. Responses of FEF pursuit neurons to passive trunk-on-head rotation with ramp trajectory. (*A*) Stimulus trajectory. (*B*) Response of 2 representative pursuit neurons. (*C*) Mean ± SE discharge of population of 53 pursuit neurons to ramp rotation. (*D*) Latency histogram of FEF pursuit neurons to velocity step trunk-on-head rotation.

with coefficient of determination (CD) = 0.91 (red line). Although trunk rotation alone induced minimal eye velocity responses (Fig. 7*B*, also Fig. 2*B*), during combined stimulation (Fig. 7*C*), eye velocity to target velocity was decreased by the mean of 18% (e.g., Fig. 7*C*) compared with the eye velocity during smooth pursuit alone (Fig. 7*A*). The thin black line in Figure 7*D* is the predicted discharge rate considering this eye velocity decrease, suggesting that smaller G during combined stimulation can be mostly due to the lower eye velocity to target velocity during combined stimulation. Of 7 neurons similarly tested, the mean G was 0.76 (±0.08SD), the mean delay τ was 10 ms (±23 SD) lag; the mean bias was –5.5 ± 6.7 SD sp/s, and the mean CD was 0.80 (±0.17 SD, range 0.54–0.94). These results indicate that discharge modulation during combined stimulation could well be predicted by the linear addition of each modulation, suggesting that neck velocity responses could indeed contribute to discharge modulation of FEF pursuit neurons during smooth pursuit if the trunk was rotated.

Comparison of Discharge Modulation during Whole-Body Rotation and Trunk-on-Head Rotation

As reported previously, the majority of FEF pursuit neurons respond to vestibular inputs induced by passive whole-body rotation during fixation of an earth-fixed target for stationary gaze (VOR ×1, Figs 1*C*, 2*C*) (Fukushima et al. 2000; Akao et al. 2007; Fukushima, Kasahara, Akao, Kurkin, et al., 2009). Mean (±SD) amplitudes of modulation of gaze-velocity neurons during passive whole-body rotation (VOR ×1) and passive trunk-on-head rotation were comparable and were 11.8 (±7.6) and 9.3 (±5.8) sp/s, respectively. Mean amplitude of modulation of eye/head-velocity neurons during passive whole-body rotation (VOR ×1) was 18.9 (±7.7 SD) sp/s and was approximately 2 times larger than the modulation during passive trunk-on-head rotation (9.6 ± 6.7 SD sp/s).

To examine how neck velocity responses and vestibular responses interact in the 2 groups of FEF pursuit neurons, Figure 5*C* and *D* plot phase and amplitudes of modulation during passive trunk-on-head rotation against those during passive whole-body rotation while the monkeys fixated an earth-fixed target. Response phases during passive trunk-on-head rotation were plotted relative to head-retrunk velocity (Figs 1*B*, 5*C*). The majority of FEF gaze-velocity neurons (26/33 = 79%) but not eye/head-velocity neurons (11/33 = 33%) exhibited opposite phase during these 2 conditions (Fig. 5*C*, + or – 45° of thin straight lines). Amplitudes of modulation of the 2 groups of neurons during passive trunk-on-head rotation and whole-body rotation were weakly but significantly correlated.

Because there was variability in both x and y values, we estimated linear regression using the orthogonal least square regression (Nyquist 1988). Slopes of linear regressions and correlation coefficients for gaze-velocity neurons were 0.53 and 0.49, respectively ($P < 0.01$). Those for eye/head-velocity neurons were 0.63 and 0.49, respectively ($P < 0.01$), and those for all tested neurons were 0.47 and 0.46, respectively ($P < 0.01$) (Fig. 5*D*, straight line). These results suggest that the neck velocity response was on the average about half of the modulation during whole-body rotation.

Modulation during Head-on-Trunk Rotation and Comparison with Modulation during Whole-Body Rotation and Trunk-on-Head Rotation

As illustrated in Figure 2*E*, the majority of FEF pursuit neurons responded to passive head-on-trunk rotation while the monkey fixated a stationary spot for stationary gaze (VOR ×1). Passive

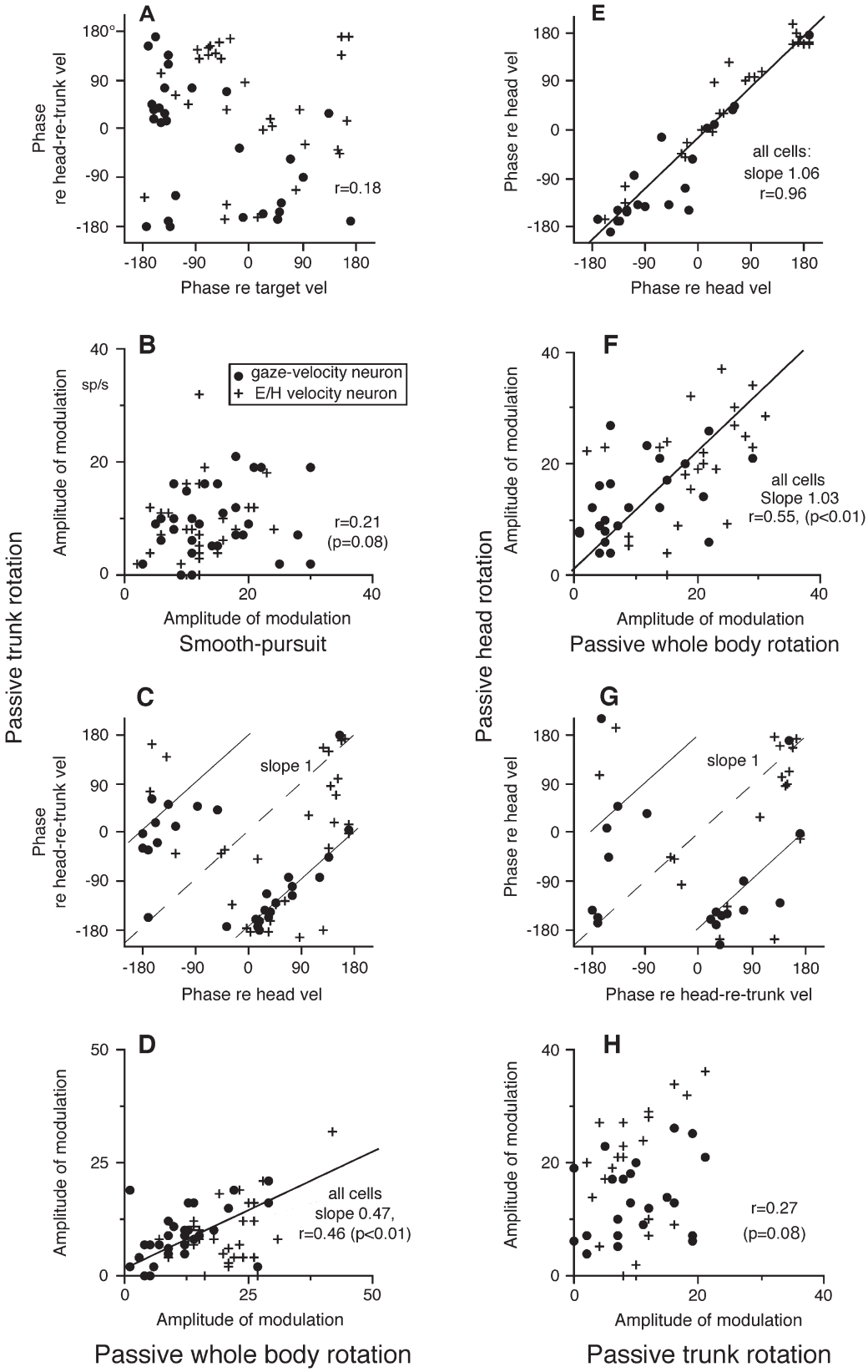

Figure 5. Comparison of discharge characteristics of FEF gaze-velocity neurons and eye/head (E/H) -velocity neurons during different tasks. (*A* and *B*) Plot phase and amplitude of modulation of the 2 groups of neurons (inset in *B*) during passive trunk-on-head rotation against those during smooth pursuit. (*C* and *D*) Plot phase and amplitude of modulation during passive trunk-on-head rotation against those during passive whole-body rotation. (*E* and *F*) Plot phase and amplitude of modulation during passive head-on-trunk rotation against those during passive whole-body rotation. (*G* and *H*) Plot phase and amplitude of modulation during passive head-on-trunk rotation against those during passive trunk-on-head rotation. Linear regressions are shown for plots with significant correlations. All data were obtained at stimulus frequency of 0.3 Hz (±10°).

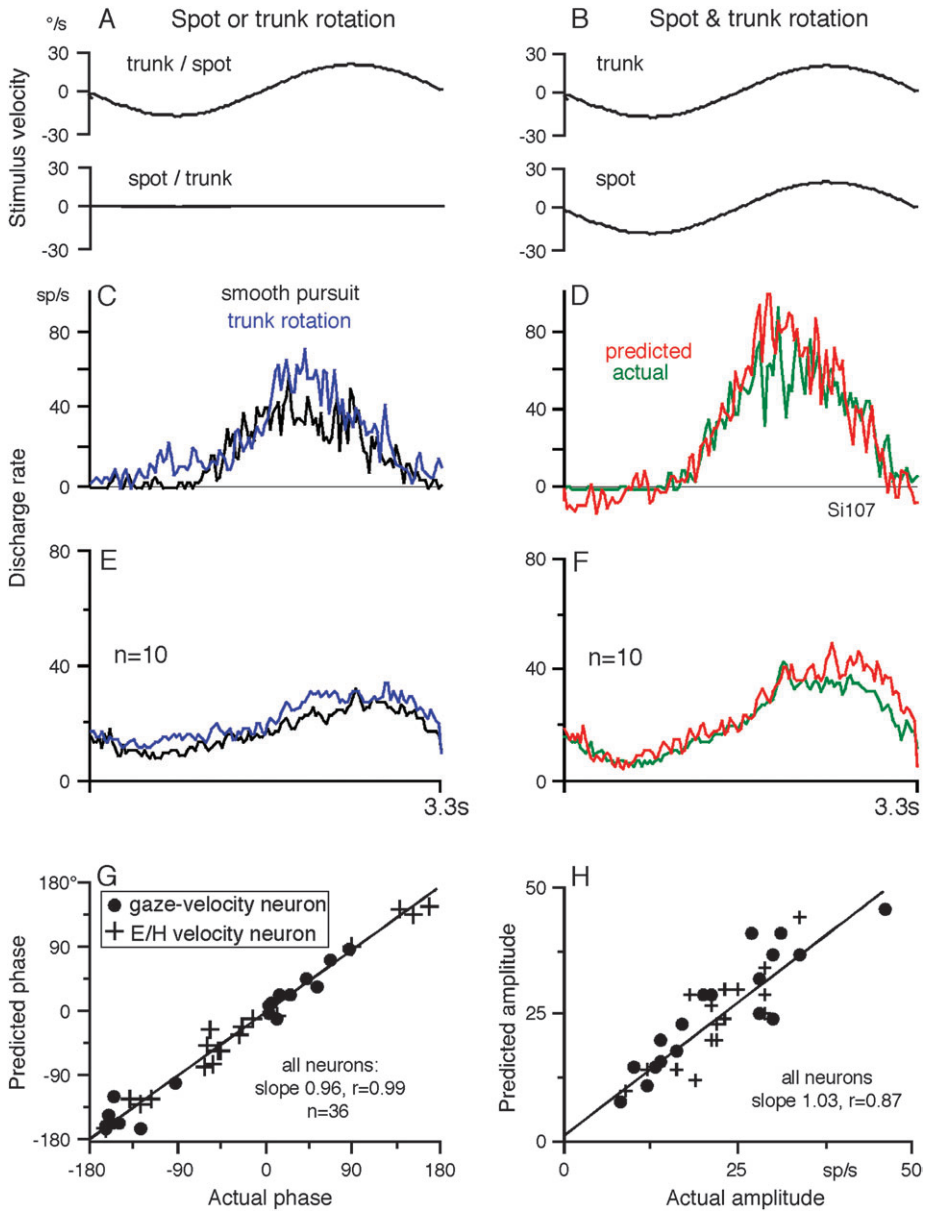

Figure 6. Linear addition of discharge modulation during smooth pursuit and passive trunk-on-head rotation. (*A*, *B*) Stimulus velocity. (*C*, *D*) and (*E*, *F*) are averaged responses of a FEF gaze-velocity neuron (*C*, *D*) and averaged population response of 10 neurons (*E*, *F*), respectively, when smooth pursuit stimulus and trunk-on-head rotation were applied separately (*C*, *E*) and when the target moved together with the trunk in the same direction with the same amplitude (*D*, *F*, green). During trunk-on-head rotation in (*C*) and (*E*), the target was stationary in space. In (*C*, *E*), neuronal responses in each condition are shown by different colors. In (*D*) and (*F*), actual modulation is shown in green. Predicted modulation is shown in red by adding responses due to 2 inputs. Resting discharge rate was subtracted from the predicted discharge. In (*G*) and (*H*), predicted responses (*G*: phase re stimulus velocity, H: amplitude of modulation) of gaze-velocity neurons and eye/head (E/H) velocity neurons (insets) are plotted against actual responses during combined stimulation. Linear regressions and regression coefficients are shown in (*G*) and (*H*) for all neurons.

head-on-trunk rotation activates both vestibular and neck proprioceptive afferents (Fig. 1*E*). Mean (±SD) amplitudes of modulation of gaze-velocity neurons and eye/head-velocity neurons to passive head-on-trunk rotation (VOR ×1) were 13.7 (±6.7) and 19.2 (±10.1) sp/s, respectively. These values were comparable to the mean amplitudes (±SD) of modulation during passive whole-body rotation (VOR ×1) which did not activate neck receptors (11.8 ± 7.6 and 18.9 ± 7.7 sp/s, respectively, for the 2 groups of neurons, see above). This is shown in Figure 5*E* and *F* that plot response phase and amplitude of modulation of each neuron during passive head-on-trunk rotation against those during whole-body rotation. The discharge modulation during the 2 conditions was correlated in both groups of neurons. The slope of linear regression coefficient and correlation coefficients for amplitude comparison for gaze-velocity neurons using the orthogonal least square regression were 0.79 and 0.48, respectively ($P < 0.02$), and those for eye/head-velocity neurons were 1.68 and 0.46, respectively ($P < 0.02$). The slope of linear regression and correlation coefficient for all tested neurons were 1.03 and 0.55 ($P < 0.01$) (Fig. 5*F*), suggesting that discharge modulation during passive head-on-trunk rotation was estimated by vestibular inputs if the activity of the 2 groups of FEF pursuit neurons was considered.

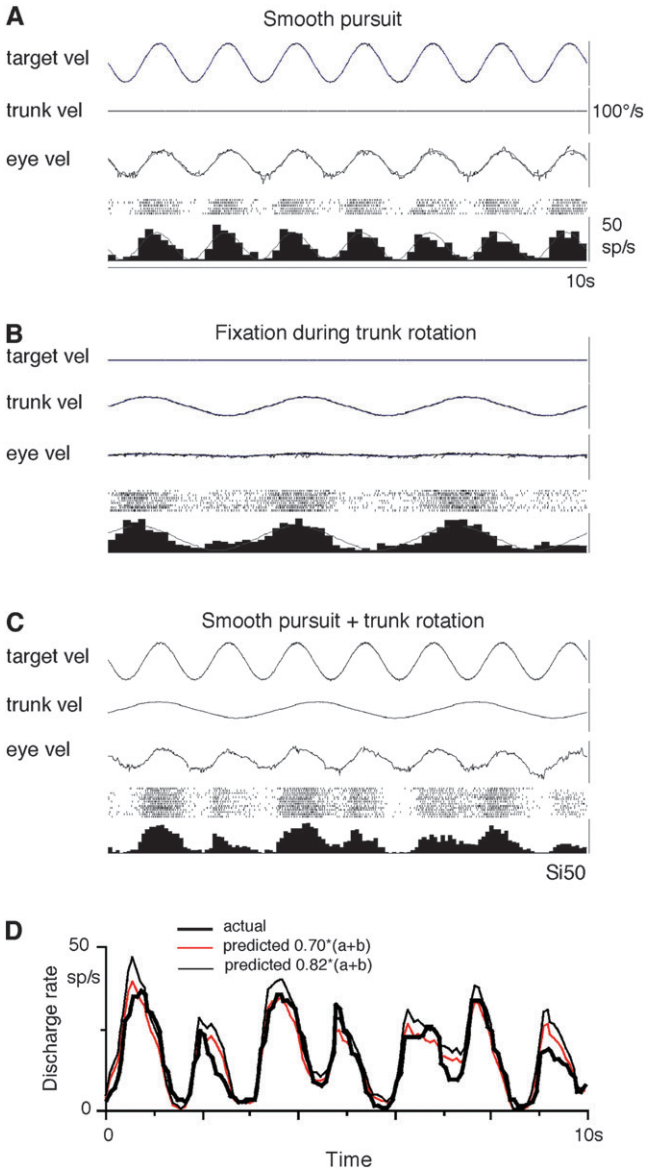

Figure 7. Linear addition of discharge modulation during smooth pursuit and passive trunk-on-head rotation in a representative FEF eye/head-velocity neuron. In (*A–C*), the top 3 traces are as indicated. The bottom 2 traces are spike rasters and averaged histograms of cell discharge during smooth pursuit at 0.7 Hz (*A*), passive trunk-on-head rotation at 0.3 Hz while the monkey fixated a stationary spot in space (*B*), and the combination of the 2 stimuli (*C*). D compares actual and predicted modulation calculated by addition of modulation in (*A*) and (*B*). In (*A*, *B*), thin lines on averaged histograms of cell discharge are superimposed fit sine waves. Eye vel indicates de-saccaded and averaged eye velocity. Target vel and trunk vel indicate target velocity in space and trunk velocity in space, respectively. For further explanation, see text.

To examine the contribution of neck velocity responses to discharge modulation induced by passive head-on-trunk rotation (Fig. 1*E*), Figure 5*G* and *H* plot response phase and amplitude of modulation during passive head-on-trunk rotation against those during trunk-on-head rotation. Many neurons that responded only weakly to trunk-on-head rotation exhibited substantial responses during passive head-on-trunk rotation (Fig. 5*H*). Using the orthogonal least square regression (Nyquist 1988), we estimated linear regression. However, significant correlation was not obtained between the 2 in gaze-velocity neurons (r = –0.22, P = 0.39), eye/head-velocity neurons (r = 0.30, P = 0.17), and all tested neurons (r = 0.27, P = 0.08, Fig. 5*H*). These results together with the significant correlation between passive head-on-trunk rotation and whole-body rotation with the slope close to one (Fig. 5*F*) suggest that discharge modulation during passive head-on-trunk rotation was estimated by vestibular inputs if the activity of the 2 groups of FEF pursuit neurons was considered (see Discussion).

Addition of Neck Velocity Responses and Vestibular Responses during Head-on-Trunk Rotation

Because passive head-on-trunk rotation activates both vestibular and neck afferents (Fig. 1*E*), we asked whether the discharge modulation during head-on-trunk rotation (VOR ×1) was predicted by the sum of modulation due to vestibular and neck velocity responses. For this, we compared actual modulation during passive head-on-trunk rotation (VOR ×1) to predicted modulation due to the 2 inputs (Fig. 1*E*). Figure 8*A–F* illustrates responses of 2 representative neurons (B–C, gaze-velocity neuron; *E–F*, eye/head-velocity neuron) when whole-body rotation (VOR ×1) and trunk-on-head rotation were given separately (*B*, *E*) and when the 2 were applied together by passive head-on-trunk rotation (*C*, *F*, actual). Both neurons increased discharge rate during rotation (trunk or whole body) towards the contralateral side (Fig. 8*A*, *B*, *D*, *E*).

During passive head-on-trunk rotation, the actual modulation of the neuron shown in Figure 8*F* (thick line) was similar to, but slightly smaller than, the modulation calculated simply by adding the 2 responses (Fig. 8*F*, thin line). In contrast, the actual modulation of the neuron shown in Figure 8*C* (thick line) during head-on-trunk rotation was different from the predicted modulation (thin line), but was similar to the modulation during whole-body rotation (Fig. 8*C* vs. 8*B*, thick lines). Consideration of off-direction saturation during the initial half cycle of whole-body rotation only slightly reduced the predicted discharge during this period (Fig. 8*C*, arrow). We compared phase and sensitivity of actual and predicted modulation (restimulus velocity) of a total of 44 neurons (20 gaze-velocity and 24 eye/head-velocity neurons) that exhibited modulation during the 2 conditions. The results are plotted in Figure 8*G,H*. Responses of the 2 example neurons (Fig. 8*A–F*) are indicated by arrows (Fig. 8*G,H*). Eye/head-velocity neurons exhibited significant correlation between predicted and actual modulation with slopes of both phase and amplitude of modulation close to one (Fig. 8*G,H*, crosses). In about half of gaze-velocity neurons, however, addition of the 2 responses suggested smaller sensitivity to head-on-trunk velocity than actual sensitivity, and phases between the 2 were considerably different (Fig. 8*G,H*, dots).

To further examine how well linear addition of vestibular and neck velocity responses predicted actual sensitivity during passive head-on-trunk rotation, ratio of actual sensitivity divided by predicted sensitivity was compared for the 2 groups of FEF pursuit neurons (Fig. 8*H*). The ratios of mean (±SD) sensitivities of eye/head-velocity neurons were close to one (0.97 ± 0.80 sp/s/°/s), indicating that the linear addition predicted actual sensitivity of eye/head-velocity neurons well. However, the ratios of mean (±SD) sensitivities of gaze-velocity neurons were 3.02 (±3.42) sp/s/°/s, clearly different from one. This was because actual sensitivity of about half of gaze-velocity neurons during head-on-trunk rotation was similar to the sensitivity

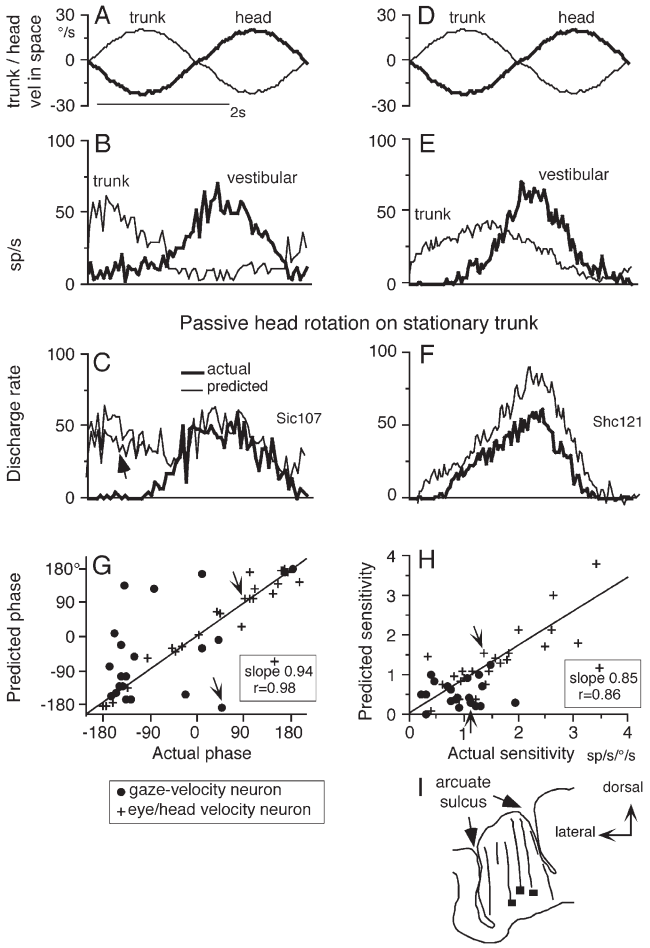

Figure 8. Linear addition of discharge modulation to neck and vestibular inputs during passive head-on-trunk rotation. (*A* and *D*) Stimulus velocity in space during trunk-on-head rotation and whole-body rotation as indicated. (*B–C*) and (*E–F*) are averaged discharge rate of 2 FEF pursuit neurons. In (*A–B*) and (*D–E*), passive trunk-on-head rotation (thin lines) and whole-body rotation (thick lines) were applied separately while, in each condition, the monkeys fixated a stationary spot in space. In (*C*) and (*F*), passive head-on-trunk rotation was applied (thick lines, actual) while the monkeys fixated a stationary target. Thin lines in (*C*) and (*F*) are predicted modulation calculated by adding neck and vestibular modulation (*B*, *E*). Directions of chair rotation during whole-body rotation (vestibular) and trunk-on-head rotation (neck, *A*, *D*) are shown oppositely, because during passive head-on-trunk rotation, neck movement direction relative to the trunk is opposite to trunk movement direction induced by chair rotation (see Fig. 1*B*, *C*). Resting discharge rate was subtracted from the predicted discharge in (*C*) and (*F*). In (*G*) and (*H*), phase (*G*) and sensitivity (*H*) of predicted modulation (restimulus velocity) that was calculated by adding neck and vestibular modulation are plotted against actual modulation (re stimulus velocity) during passive head-on-trunk rotation for gaze-velocity neurons and eye/head-velocity neurons. (*I*) Transverse section of representative recording tracks of monkey Si and locations of 3 pursuit neurons responding to trunk-on-head rotation (squares). For further explanation, see text.

during whole-body rotation (e.g., Fig. 8*B* vs. 8*C*, thick lines). The significance of this finding will be considered in the Discussion.

Recording Locations

As illustrated in Figure 8*I*, recording locations were within the caudal part of the arcuate sulcus primarily in the fundus, similar to the locations in previous studies (e.g., MacAvoy et al. 1991; Gottlieb et al. 1993; Tanaka and Fukushima 1998; Fukushima et al. 2000). Another monkey is still being used. However, because of our extensive experience with the characteristic discharge properties of pursuit neurons in the caudal FEF and the similarity in the recording locations in stereotaxic coordinates as reported previously, we are confident that recordings in this monkey also were from similar areas (also Fukushima, Yamanobe, Shinme, Fukushima, 2002; Fukushima, Yamanobe, Shinme, Fukushima, Kurkin, et al. 2002; Akao et al. 2005, 2007, 2009; Kurkin et al. 2007, 2009).

Discussion

Primary Source of Neck Velocity Responses of FEF Pursuit Neurons during Passive Trunk-on-Head Rotation: Neck Proprioceptive Responses

Our results demonstrate for the first time that the majority (69/79 = 87%) of horizontal pursuit neurons in the caudal FEF responded to passive trunk-on-head rotation (Figs 2–4). Neck velocity responses were observed in both gaze-velocity neurons and eye/head-velocity neurons tested with similar percentage (31/33 and 30/33) and with similar amplitudes (mean ± SD, 9.3 ± 5.8 and 9.6 ± 6.7 sp/s, respectively). For the following reasons, we conclude that this modulation was induced primarily by neck proprioceptive inputs. 1) The modulation during passive trunk-on-head rotation cannot reflect eye movement responses (i.e., cervico-ocular reflex, COR), because eye velocity responses to trunk-on-head rotation were negligible (Figs 2*B*, 7*B*). 2) It is unlikely that the modulation reflected active head movement commands resisting trunk-on-head rotation or motor corollary, because our recent studies in the same monkeys during active head-free pursuit have shown that FEF pursuit neurons were unlikely to issue a head-pursuit command; rather they carried primarily eye-pursuit signals and re-afferent signals resulting from head movements (Fukushima, Kasahara, Akao, Kurkin, et al. 2009). 3) It is unlikely that the modulation was induced by tactile afferents of the neck skin, because none of 10 neurons tested exhibited a clear response to tactile stimulation of the neck skin. 4) Finally, it is well known that passive trunk-on-head rotation is an effective way to activate neck proprioceptive afferents (e.g., Peterson 1988; Gdowski and McCrea 2000; Gdowski et al. 2001).

Although the cervical vertebral joint afferents were classically thought as the source of neck proprioceptive afferents, later studies have revealed that neck muscle spindles are the primary source that signals head movements relative to the trunk (see Peterson 1988 for a review). The present studies have shown that responses induced by passive trunk-on-head rotation consisted primarily of velocity components and some position and acceleration components (Fig. 4*A–C*). FEF pursuit neurons that carried only a position component were in the minority (3/53 = 6%). These responses are consistent with the idea that they were induced by neck muscle spindles (Peterson 1988).

Neck afferent signals have been shown in parietotemporal cortex in cats (Kornhuber 1972) and monkeys (parieto-insular vestibular cortex [PIVC], Grüsser et al. 1990; lateral intraparietal sulcus LIP and area 7a, Snyder et al. 1998; ventral intraparietal sulcus VIP, Avillac et al. 2005), and in PIVC and premotor cortex in humans (Bottini et al. 2001). Specifically, studies on the neural activity in LIP and VIP where eye movement–related neurons are found have reported the importance of head *position* relative to the trunk for representation of visual and tactile signals (e.g., Snyder et al.

1998; Avillac et al. 2005), but none of them reported neck *velocity* signals. The great majority of FEF pursuit neurons in the present study responded primarily to *velocity* of head-motion relative to the trunk (Fig. 4*C*). This suggests that hitherto unexplored sites in the brain might also encode neck velocity.

Interaction of Neck Proprioceptive and Vestibular Responses in FEF Pursuit Neurons

The importance of neck proprioceptive signals for reflex stabilization of the head and trunk is well known (Peterson 1988). These signals are believed to contribute to the COR in squirrel monkeys, where the gain of the COR is high (0.4 at 0.5 Hz, Gdowski and McCrea 2000). In rhesus macaques and humans, however, neck movement driven eye movements are known to be small (e.g., Dichgans et al. 1973), similar to the COR gain of macaque monkeys (*M. fuscata*) in the present study (<0.1 at 0.3 Hz, Figs 2*B*, 7*B*).

In squirrel monkeys, discharge modulation due to neck proprioceptive inputs and vestibular inputs add linearly and antagonistically in most second order vestibular neurons. As a result, the vestibular responses of individual neurons during passive head-on-trunk rotation are reduced (Gdowski and McCrea 2000). Second order vestibular neurons include neurons that send signals to the FEF through the thalamus (Ebata et al. 2004; Akao et al. 2007). The present results show that, in the FEF, the preferred directions (relative to head-retrunk velocity) of neck proprioceptive responses of the majority of pursuit neurons, especially those of gaze-velocity neurons, were antagonistic to those of vestibular responses (Figs 5*C*, 8*B*), similar to second order vestibular neurons (Gdowski and McCrea 2000). This result suggests that the brainstem source for neck proprioceptive responses in the FEF may come through the ascending vestibular pathway in which vestibular and neck responses have already converged. However, previous studies have reported that pursuit-related neurons in the vestibular nuclei of rhesus monkeys do not carry neck proprioceptive signals (Roy and Cullen 2003), suggesting that neck proprioceptive signals must also be conveyed through pathways separate from eye movement–related ascending vestibular pathways. Neck proprioceptive signals are also known to be conveyed through the somato-sensory pathway (Abrahams et al. 1984; see Peterson 1988 for a review). These signals could then be conveyed through cortico-cortical pathways to the FEF (Guldin et al. 1992; Stanton et al. 2005).

In eye/head-velocity neurons and about half of gaze-velocity neurons in the caudal FEF, our results indicate that discharge modulation during passive head-on-trunk rotation was predicted well by linear addition of neck proprioceptive responses and vestibular responses (Fig. 8*G*,*H*). However, in the remaining half of gaze-velocity neurons, actual sensitivity during head-on-trunk rotation was larger than predicted modulation by linear addition (Fig. 8*H*). This was because the actual discharge was not reduced as predicted by linear addition of the 2 antagonistic responses (Figs. 5*C*,8*C*). Rather, unlike vestibular neurons of squirrel monkeys (Gdowski and McCrea 2000), neck responses did not appear during passive head-on-trunk rotation (VOR ×1) in these gaze-velocity FEF neurons and the actual responses were similar to vestibular responses induced by whole-body rotation (also Fig. 5*F*). This nonlinear summation suggests that, in these gaze-velocity FEF neurons, neck responses were suppressed in the presence of vestibular inputs during head-on-trunk rotation (also Fig. 5*H*, see below).

Possible Role of Neck Proprioceptive Signals in the Caudal FEF

The importance of neck proprioceptive signals in the cerebral representation of egocentric space has been suggested (Bottini et al. 2001; Karnath and Dieterich 2006). Neck movement signals are necessary for representation of visual and tactile signals in body-centered coordinates (Mergner et al. 1998), and are observed in neurons in LIP and VIP (Snyder et al. 1998; Avillac et al. 2005). The present results indicate that the majority of FEF pursuit neurons exhibited neck velocity responses signaling the direction of head rotation relative to the trunk, in addition to vestibular responses signaling the direction of whole-body rotation and visual responses signaling target motion as reported earlier (Fukushima et al. 2000; Fukushima, Yamanobe, Shinme, Fukushima, 2002; Akao et al. 2005, 2007). Thus, like VIP neurons (e.g., Schlack et al. 2003; Avillac et al. 2005), FEF pursuit neurons carried multimodal signals. However, unlike VIP neurons that discharge after the onset of smooth pursuit eye movements (Schlack et al. 2003), the majority of FEF pursuit neurons discharge before the onset of pursuit eye movements, which suggests a pursuit command (MacAvoy et al. 1991; Gottlieb et al. 1993; Tanaka and Fukushima 1998; Fukushima, Yamanobe, Shinme, Fukushima, Kurkin, et al. 2002; Akao et al. 2005, 2007; Fukushima et al. 2008; Kurkin et al. 2009).

By comparing preferred directions of FEF pursuit neurons in head- and trunk-restrained monkeys during upright and static whole-body roll-tilt, the FEF has been shown to code pursuit signals in head/trunk-centered (but not earth-vertical) coordinates (Kurkin et al. 2007). The present results showing that modulation induced by passive trunk-on-head rotation added linearly with modulation during smooth pursuit (Figs 6, 7) further suggest that neck proprioceptive signals could contribute to representing pursuit signals with respect to the trunk if the head moves relative to the trunk. The modal latency of 35 ms would be short enough for neck proprioceptive signals to influence pursuit-related discharge during rapid rotation of the trunk under the stationary head (Fig. 4*D*). Addition of vestibular modulation during passive head-on-trunk rotation in a majority of FEF pursuit neurons (Fig. 8) could allow representation of gaze signals in the FEF with respect to the trunk. The 2 neurons in Figure 2*F* do in fact exhibit such signals during gaze movement on the stationary trunk.

We come finally to the complex interactions between neck proprioceptive and vestibular signals that were shown in Figure 8*A*–*H*. In both of our monkeys about half of the FEF gaze-velocity neurons responded vigorously to neck rotation when it was delivered by rotating the body beneath a fixed head but much more weakly when such rotation occurred as part of forced rotation of the head on the trunk (Fig. 8*B*–*C*, *H*). This finding clearly shows that neck proprioceptive signals reaching FEF pursuit neurons can be strongly influenced by the context in which neck rotation occurs (also Fig. 5*H*). Note that this effect (Fig. 8*B*, *C*, *H*) is only present in 1 of the 2 functional classes of FEF pursuit neurons (i.e., gaze-velocity, but not eye/head-velocity neurons). This reinforces the notion that gaze-velocity and eye/head-velocity neurons are distinct classes

within the pursuit region of the FEF (Fukushima et al. 2000; Akao et al. 2007; Fukushima, Kasahara, Akao, Kurkin, et al., 2009). It would be interesting to determine the projection(s) of these 2 types of neurons.

At present we can only speculate about the possible roles the neck inputs to eye/head and gaze-velocity neurons might play. We think that neck inputs could contribute to representing target-, eye-, and gaze-velocity in trunk coordinates in context-dependent manner. Where both eye/head-velocity and gaze-velocity signals are active during head-on-trunk rotation, they tend to combine in a way that generates a target velocity with respect to trunk signal. In the case of gaze-velocity neurons that do not exhibit suppression of the neck signals this would lead to a *gaze with respect to trunk signal*. This would be useful in contexts where the animal was following a target that moved with his body (eye-hand coordination for instance, e.g., Maioli et al. 2007). Animals also have to follow targets in the external world. Gaze-velocity neurons where the neck rotation signal is suppressed during head-on-trunk rotations would serve this purpose.

Activity of eye/head-velocity neurons does not change greatly when an animal stabilizes its gaze using the VOR as opposed to active pursuit. In both cases, the neurons' discharge follows velocity of the eye in the orbit. The neck input received by all of these neurons during passive head-on-trunk rotation tends to convert this to an *eye velocity with respect to trunk signal*. This could be useful for signaling required smooth eye velocity with respect to the trunk velocity during head-on-trunk rotation. We have shown earlier that pursuit signals are represented 3 dimensionally (3D) in the FEF by combining fronto-parallel pursuit (i.e., smooth pursuit) and vergence pursuit velocity components (Fukushima, Yamanobe, Shinme, Fukushima, Kurkin, et al. 2002) Representation of pursuit velocity signals relative to trunk velocity during head movement would be useful for coordination of pursuit eye movements with hand and/or arm movements for reaching a moving target in 3D extrapersonal space.

Funding

Grant-in-Aid for Scientific Research on Priority Areas (System study on higher-order brain functions) (17022001) and (C) (20500351) from the MEXT of Japan.

Notes

We thank Dr Tim Belton for his valuable comments on the manuscript. *Conflict of Interest*: None declared.

Address correspondence to Kikuro Fukushima, MD, DMS, Department of Physiology, Hokkaido University School of Medicine, West 7, North 15, Sapporo, Hokkaido, 060-8638 Japan. Email: kikuro@med.hokudai.ac.jp.

References

Abrahams VC, Richmond FJ, Keane J. 1984. Projections from C2 and C3 nerves supplying muscles and skin of the cat neck: a study using transganglionic transport of horseradish peroxidase. J Comp Neurol. 230:142–154.

Akao T, Kurkin S, Fukushima J, Fukushima K. 2005. Visual and vergence eye movement related responses of pursuit neurons in the caudal frontal eye fields to motion-in-depth stimuli. Exp Brain Res. 164:92–108.

Akao T, Kurkin S, Fukushima J, Fukushima K. 2009. Otolith inputs to pursuit neurons in the frontal eye fields of alert monkeys. Exp Brain Res. 193:455–466.

Akao T, Saito H, Fukushima J, Kurkin S, Fukushima K. 2007. Latency of vestibular responses of pursuit neurons in the caudal frontal eye fields to whole body rotation. Exp Brain Res. 177:400–410.

Avillac M, Deneve S, Olivier E, Pouget A, Duhamel J-R. 2005. Reference frames for representing visual and tactile locations in parietal cortex. Nat Neurosci. 8:941–949.

Bottini G, Karnath HO, Vallar G, Frith CD, Frackowiak RSJ, Paulesu E. 2001. Cerebral representations for egocentric space: functional-anatomical evidence from caloric vestibular stimulation and neck vibration. Brain. 124:1182–1196.

Dichgans J, Bizzi E, Morasso P, Tagiasco V. 1973. Mechanisms underlying recovery of eye-head coordination following bilateral labyrinthectomy in monkeys. Exp Brain Res. 18:548–562.

Ebata S, Sugiuchi Y, Izawa Y, Shinomiya K, Shinoda Y. 2004. Vestibular projection to the periarcuate cortex in the monkey. Neurosci Res. 49:55–68.

Fuchs AF, Robinson DA. 1966. A method for measuring horizontal and vertical eye movements chronically in the monkey. J Appl Physiol. 21:1068–1070.

Fukushima K, Akao T, Saito H, Kurkin S, Fukushima J, Peterson BW. 2007. Neck proprioceptive signals in pursuit neurons in the frontal eye fields (FEF) of monkeys. Program No. 398.5. Abstract Viewer/Itinerary Planner. San Diego (CA): Society for Neuroscience, Washington, D.C.

Fukushima K, Sato T, Fukushima J, Shinmei Y, Kaneko CRS. 2000. Activity of smooth pursuit-related neurons in the monkey periarcuate cortex during pursuit and passive whole body rotation. J Neurophysiol. 83:563–587.

Fukushima K, Yamanobe T, Shinmei Y, Fukushima J. 2002. Predictive responses of peri-arcuate pursuit neurons to visual target motion. Exp Brain Res. 145:104–120.

Fukushima K, Yamanobe T, Shinmei Y, Fukushima J, Kurkin S, Peterson BW. 2002. Coding of smooth eye movements in three-dimensional space by frontal cortex. Nature. 419:157–162.

Fukushima K, Akao T, Shichinohe N, Nitta T, Kurkin S, Fukushima J. 2008. Predictive signals in the pursuit area of the monkey frontal eye fields. Prog Brain Res. 171:433–440.

Fukushima K, Kasahara S, Akao T, Kurkin S, Fukushima J, Peterson BW. 2009. Eye-pursuit and re-afferent head movement signals carried by pursuit neurons in the caudal part of the frontal eye fields during head-free pursuit. Cereb Cortex. 19:263–275.

Fukushima K, Kasahara S, Akao T, Saito H, Kurkin S, Fukushima J, Peterson BW. 2009. Re-afferent head movement signals carried by pursuit neurons in the simian frontal eye fields during head movements. Ann N Y Acad Sci. 1164:194–200.

Gdowski GT, Belton T, McCrea RA. 2001. The neurophysiological substrate for the cervico-ocular reflex in the squirrel monkey. Exp Brain Res. 140:253–264.

Gottlieb JP, Bruce CJ, MacAvoy MG. 1993. Smooth eye movements elicited by microstimulation in the primate frontal eye field. J Neurophysiol. 69:786–799.

Gottlieb JP, MacAvoy MG, Bruce CJ. 1994. Neural responses related to smooth pursuit eye movements and their correspondence with electrically elicited slow eye movements in the primate frontal eye field. J Neurophysiol. 72:1634–1653.

Gdowski GT, McCrea RA. 2000. Neck proprioceptive inputs to primate vestibular nuclear neurons. Exp Brain Res. 135:511–526.

Grüsser O-J, Pause M, Schreiter U. 1990. Vestibular neurones in the parieto-insular cortex of monkeys (Macaca fascicularis): visual and neck receptor responses. J Physiol. 430:559–583.

Guldin WO, Akbarian S, Grüsser O-J. 1992. Cortico-cortical connections and cytoarchitectonics of the primate vestibular cortex: a study in squirrel monkeys (Saimiri sciureus). J Comp Neurol. 326:375–401.

Karnath HO, Dieterich M. 2006. Spatial neglect-a vestibular disorder? Brain. 129:293–305.

Kasahara S, Akao T, Fukushima J, Kurkin S, Fukushima K. 2006. Further evidence for selective difficulty of upward eye pursuit in young monkeys: effects of optokinetic stimulation, static roll tilt, and active head movements. Exp Brain Res. 171:306–321.

Kornhuber HH. 1972. Vestibular influences on the vestibular and the somatosensory cortex. Prog Brain Res. 37:567–572.

Kurkin SA, Akao T, Fukushima J, Fukushima K. 2007. Activity of pursuit neurons in the caudal part of the frontal eye fields during static roll-tilt. Exp Brain Res. 176:685–664.
Kurkin S, Akao T, Fukushima J, Fukushima K. 2009. Discharge of pursuit-related neurons in the caudal part of the frontal eye fields in juvenile monkeys with up-down pursuit asymmetry. Exp Brain Res. 193:181–188.
Leigh R, Zee DS. 2006. The neurology of eye movements. 4th ed. New York: Oxford University Press.
Lisberger S, Fuchs AF. 1978. Role of primate flocculus during rapid behavioral modification of vestibuloocular reflex. I. Purkinje cell activity during visually guided horizontal smooth-pursuit eye movements and passive head rotation. J Neurophysiol. 41:733–763.
MacAvoy MG, Gottlieb JP, Bruce CJ. 1991. Smooth pursuit eye movement representation in the primate frontal eye field. Cereb Cortex. 1:95–102.
Maioli C, Falciati L, Gianesini T. 2007. Pursuit eye movements involve a covert motor plan for manual tracking. J Neurosci. 27:7168–7173.
Mergner T, Nasios G, Anastasopoulos D. 1998. Vestibular memory-contingent saccades involve somatosensory input from the body support. Neuroreport. 9:1469–1473.
Mergner T, Rottler G, Kimming H, Becker W. 1992. Role of vestibular and neck inputs for the perception of object motion in space. Exp Brain Res. 89:655–668.
Nyquist H. 1988. Least orthogonal absolute deviations. Comput Stat Data Anal. 6:361–367.
Peterson BW. 1988. Cervicocollic and cervicoocular reflexes. In: Peterson BW, Richmond FJ, editors. Control of head movement. New York: Oxford University Press.
Roy JF, Cullen KE. 2003. Brain stem pursuit pathway: dissociating visual, vestibular, and proprioceptive inputs during combined eye-head gaze tracking. J Neurophysiol. 90:271–290.
Schlack A, Hoffmann KP, Bremmer F. 2003. Selectivity of macaque ventral intraparietal area (area VIP) for smooth pursuit eye movements. J Physiol. 551:551–561.
Singh A, Thau GE, Raphan T, Cohen B. 1981. Detection of saccades by a maximum likelihood ratio criterion. Proc 34th Ann Conf Eng Biol, Houston, TX: 136.
Snyder LH, Grieve KL, Brotchie P, Andersen RA. 1998. Separate body- and world-referenced representations of visual space in parietal cortex. Nature. 394:887–891.
Stanton GB, Friedman HR, Dias EC, Bruce CJ. 2005. Cortical afferents to the smooth-pursuit region of the macaque monkey's frontal eye field. Exp Brain Res. 165:179–192.
Tanaka M, Fukushima K. 1998. Neuronal responses related to smooth pursuit eye movements in the periarcuate cortical area of monkeys. J Neurophysiol. 80:28–47.
Wilson VJ, Ezure K, Timerick SJB. 1984. Tonic neck reflex of the decerebrate cat: response of spinal interneurons to natural stimulation of neck and vestibular receptors. J Neurophysiol. 51:567–577.